

Target Thermo-Mechanical Behavior During Injection in the LIFE Engine

Progress report #1

M. S. Tillack, X. R. Wang and D. S. Holdener

12 November 2009



Target Thermo-Mechanical Behavior During Injection in the LIFE Engine

Progress Report

10 November 2009

M. S. Tillack, X. R. Wang, D. S. Holdener
Center for Energy Research
UC San Diego

Introduction

We have assessed modeling techniques and performed analysis of the basic fluid and thermal behavior of a LIFE hohlraum traveling through the post-blast chamber environment. Our initial effort has focused on the survival of the laser entrance hole (LEH) window. We find that a polyimide window could survive, but the design window is narrow. Design choices can help expand the window, but we also find it critically important to establish accurate properties (like radiation emissivity of polyimide) and verify the heat transfer coefficient, h . Different computational models predict values of h that are so different that the survival of the LEH window depends on which is correct. More research into the validity of turbulent finite element codes and direct simulation Monte Carlo codes in this regime is warranted. Experimental verification may ultimately be needed.

Two methods are available for solving the fluid and thermal behavior of injected targets: direct simulation molecular dynamics (Monte Carlo) and continuum fluid (Navier-Stokes) finite element codes. This happy situation arises from the fact that the Knudsen number is small enough to be treated as a viscous fluid, whereas the particle number density is low enough that a Monte Carlo solution is tractable on a modern PC platform. For the conditions listed in Table 1, the stream mean-free-path is $53.8 \mu\text{m}$ (computed by DS2V) and the Knudsen number based on radius is 0.016.

DS2V [3] is a well-established 2D direct simulation Monte Carlo code with a friendly graphical input/output user interface. The computer models a real gas by some thousands or millions of simulated molecules. The velocity components and position coordinates of these molecules are stored in the computer and are modified with time as the molecules are concurrently followed through representative collisions and boundary interactions in simulated physical space. Personal computers now readily permit DSMC calculations of two-dimensional and axially symmetric flows at overall Knudsen numbers in the range 0.01 to 0.001, which is well into the continuum regime. On the other hand, continuum codes show significant errors when local Knudsen numbers exceed 0.1 and are hardly useable when they exceed 0.2.

Two continuum codes were tested: ANSYS CFX and COMSOL. The primary advantage of these codes is their ability to simultaneously analyze radiation heat transfer and structural responses as well as thermal and fluid responses. The primary disadvantage is their limitation to continuum flow regimes. One goal of this work is to quantify differences between continuum and Monte Carlo codes in this flow regime.

For this work we assumed a common set of target parameters [1] and chamber parameters [2] that are summarized in Table 1.

Table 1. Reference parameters used in the analyses (37.5 MJ LIFE target)

| | |
|--------------------------------|-------------------------------|
| Hohlraum radius | 3.3 mm |
| Hohlraum length | 11.9 mm |
| Window material | Polyimide (Kapton) |
| Window thickness | 0.5 μm |
| Hohlraum wall material | Lead |
| Hohlraum wall thickness | 25 μm |
| Chamber gas | Xenon |
| Chamber gas density | $2 \times 10^{22}/\text{m}^3$ |
| Chamber gas temperature | 1000 °K |
| Chamber gas pressure at Tg | 350 Pa |
| Target injection velocity | 200 m/s |
| Target transit distance in gas | 5 m |
| Initial target temperature | 20 K |

Heat transfer coefficients using DS2V

In the current LIFE reference target design, a polyimide laser entrance hole (LEH) window is embedded into the two faces of the hohlraum (see Figure 1). In order to evaluate the heating of the window, one of the most important parameters is the heat transfer coefficient from the chamber gas to the hohlraum surfaces. To determine this we modeled the hohlraum in DS2V using “diffuse reflection with full accommodation” for the surface interaction model (this is the only free parameter in the simulations). The geometry of the reference target is a perfect right cylinder. Later we explore the effect of rounded corners and rounded faces.

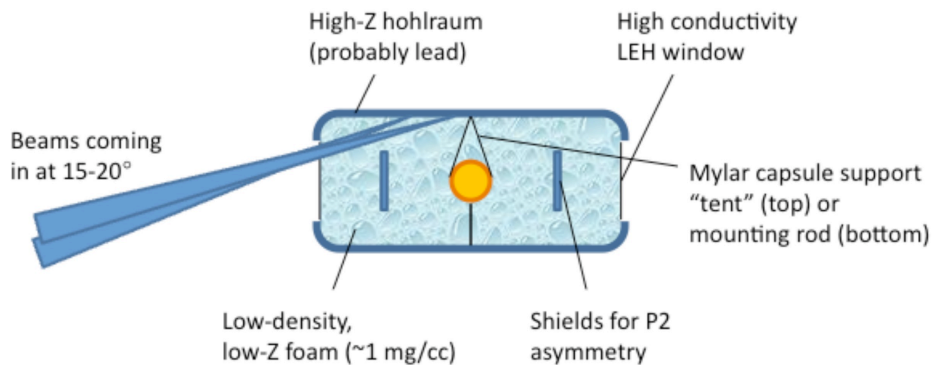


Figure 1. Hohlraum geometry

Figures 2 and 3 depict the flow speed and heat transfer coefficient for this case. The abscissa on the heat transfer coefficient graph follows the surface from the leeward side to the windward side. A difference of a factor of 10 can be seen from back to front, with the front corner the

highest at 2.6 W/cm^2 . With a 1000 K temperature difference, the heat transfer coefficient is $26 \text{ W/m}^2\text{K}$ at the leading corner where the flow is highest.

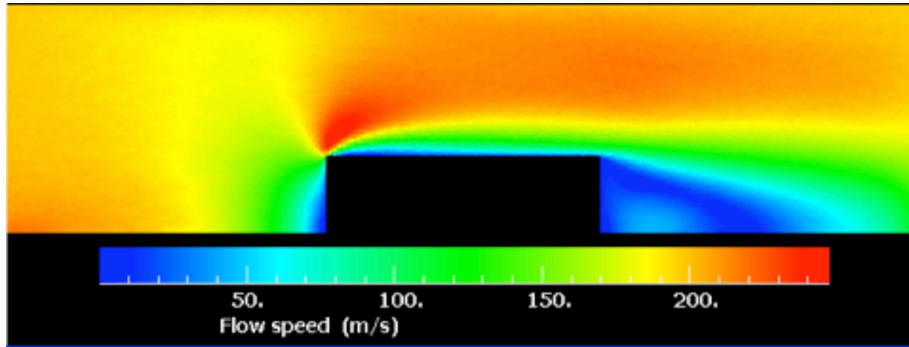


Figure 2. Flow speed around the hohlraum with 200 m/s injection velocity

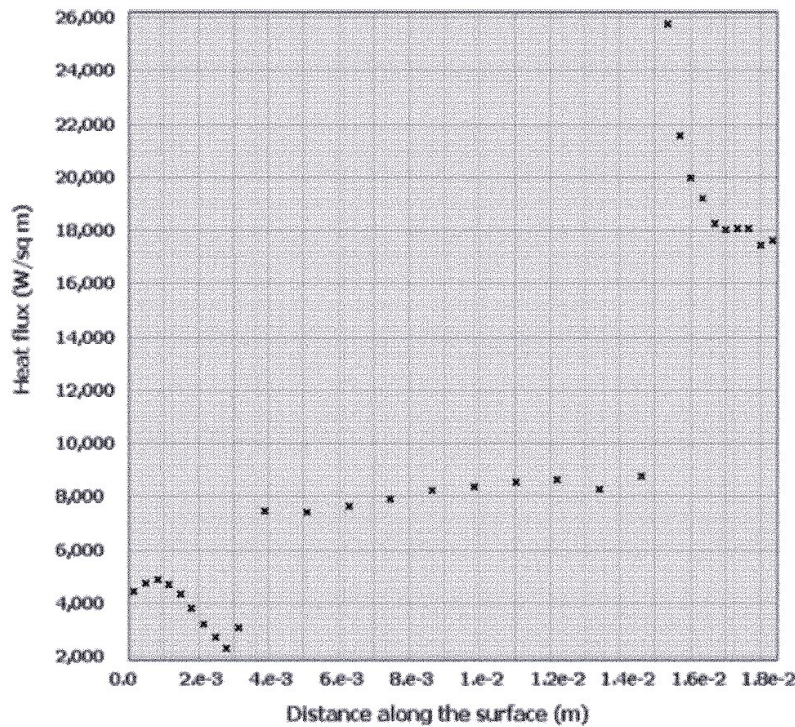


Figure 3. Heat transfer around the surface of the hohlraum with 200 m/s injection velocity (starting at the leeward center and ending at the windward center)

Heat transfer coefficients from correlations

To check the “order of magnitude” validity of these modeling results, we explored standard heat transfer coefficients from the literature. On page 370 of Incropera and DeWitt [4], a general heat transfer coefficient over cylinders in cross flow is given by:

$$\text{Nu} = hD/k_f = C \text{Re}^m \text{Pr}^{1/3} \quad (1)$$

This was applied to the case of an infinitely deep flat plate with impinging flow and a rectangular cylinder, as shown in cross section in Figure 4. Parameters used in the evaluation of this correlation are listed in Table 2.

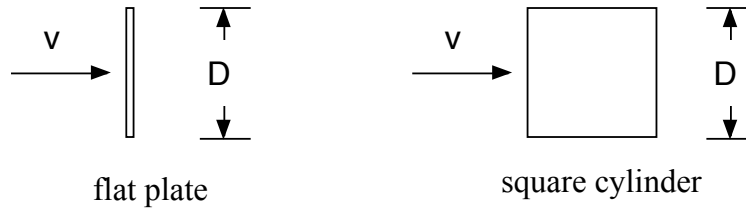


Figure 4. Cross sections of two geometries used to estimate the Nusselt number

Table 2. Parameters used in the evaluation of the Nusselt number

| | | |
|--------|------|-----------------------------|
| C_p | 160 | J/kg-K |
| μ | 76 | $\mu\text{Pa}\cdot\text{s}$ |
| k_f | 0.01 | W/m-K |
| Pr | 1.22 | $(C_p\mu/k)$ |
| ρ | 4.36 | g/m^3 |
| v | 200 | m/s |
| D | 6.6 | mm |
| Re | 75.7 | $(\rho v D/\mu)$ |

For a vertical plate, this expression can be used with $C=0.228$ and $m=0.731$ (valid for $4 \times 10^3 < \text{Re} < 1.5 \times 10^4$). In our case, $\text{Re}=75.7$, which is technically outside the range of validity. Evaluating the Nusselt number and heat transfer coefficient on the front surface using this correlation gives $8.7 \text{ W}/\text{m}^2\text{K}$, which is about a factor of 2 lower than the DS2V calculation.

For a square cross-section cylinder in cross flow, the expression above can be used with $C=0.102$ and $m=0.675$ (valid for $5 \times 10^3 < \text{Re} < 10^5$). In this case, the heat transfer coefficient is averaged around the perimeter of the cylinder. Averaging the heat flux values in Figure 2 predicts a heat transfer coefficient of approximately $9 \text{ W}/\text{m}^2\text{K}$, whereas the semi-empirical correlation predicts $3.1 \text{ W}/\text{m}^2\text{K}$. Again, the semi-empirical correlation predicts a significantly lower value than DS2V.

Heat transfer coefficients from finite element codes

A detailed 3D CFD thermal-fluid analysis was performed using ANSYS CFX to explore the fluid dynamic behavior and to compare the results obtained by DS2V. A 5-degree slice of a hohlraum target was considered in the CFD model and the hohlraum target was surrounded by xenon gas. A standard $k-\epsilon$ turbulent flow model with smooth walls was assumed in the CFD simulation. Figure 5 shows the velocity distribution of the gas around the hohlraum target and Figure 6 shows the heat transfer coefficient at the interface of the Xe and hohlraum target.

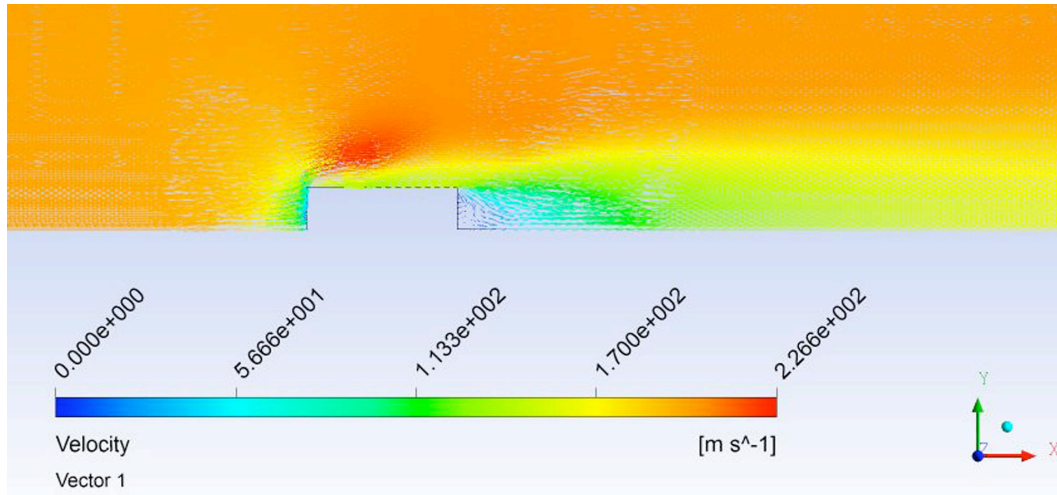


Figure 5. Velocity distribution around the target predicted by ANSYS

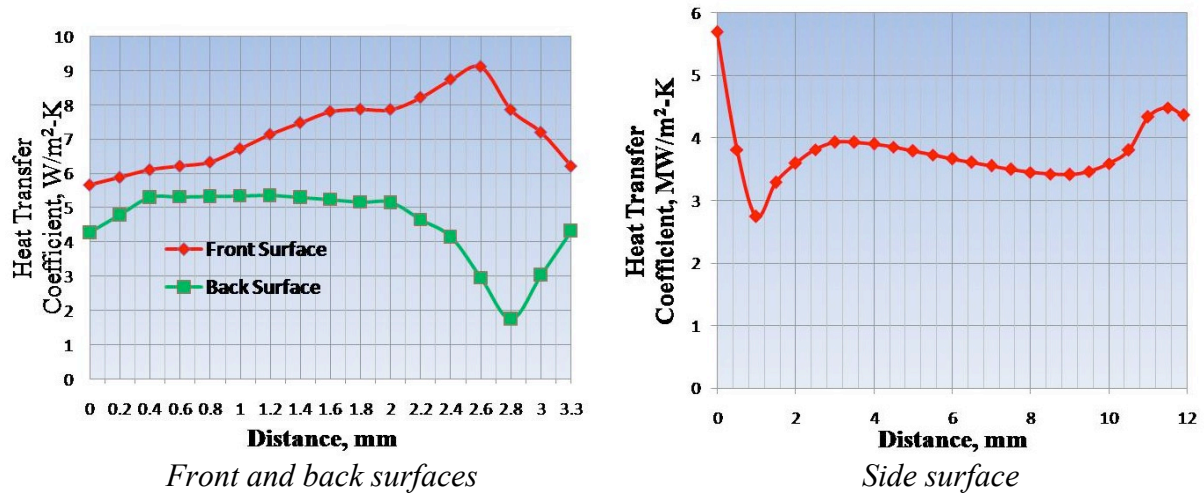


Figure 6. Heat transfer coefficient at the interface of the target and Xe predicted by ANSYS

The flow field is qualitatively very similar to the result from DS2V. On the other hand, the heat transfer coefficient peaks at about $9 \text{ W/m}^2\text{-K}$. This agrees well with the semi-empirical correlation for viscous flow around a flat plate, about a factor of 3 lower than DS2V.

Comsol also was used to perform a similar analysis. In this case, a 2D axisymmetric geometry was created. Again a $k-\epsilon$ turbulent flow model was employed. The results are shown in Figures 7 and 8. The results are very similar to ANSYS. There is strong evidence that a turbulent viscous model of the flow field yields a consistent result of $9 \text{ W/m}^2\text{-K}$ peak heat transfer coefficient, in contrast to the results of direct Monte Carlo simulations.

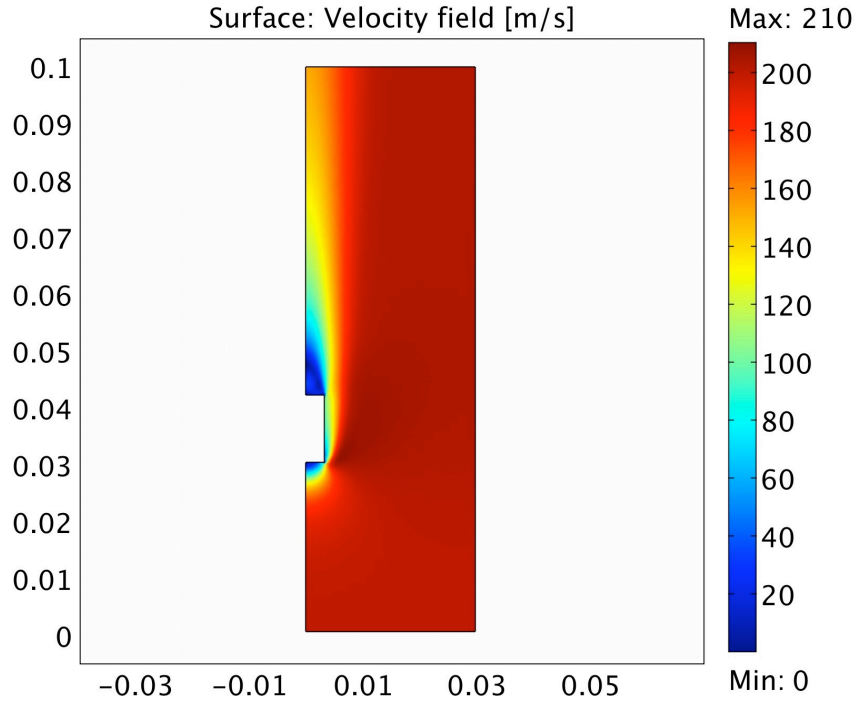


Figure 7. Velocity distribution around the target predicted by COMSOL

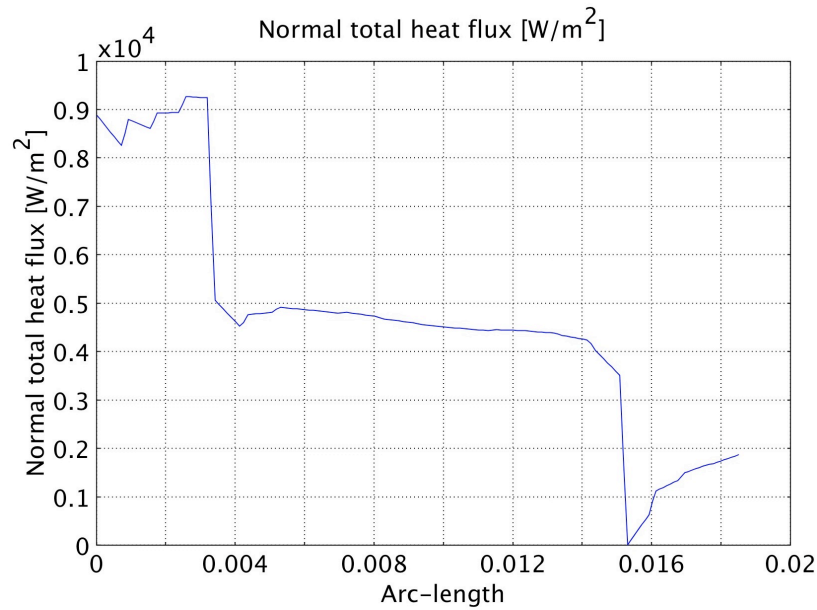


Figure 8. Heat transfer coefficient at the interface of the target and Xe predicted by COMSOL

Polyimide heating

Using these heat transfer coefficients, a full transient thermal analysis of the LEH window can be performed. Before doing so, it is instructive to calculate the Biot number (hL/k_s) of this mixed conduction/convection problem. Although the thermal conductivity of polyimide is low (around 0.05 W/m-K), the thickness is so small that the Biot number is still small – around 2×10^{-4} . This means conduction within the window is much faster than convection from the gas, such that the window can be assumed isothermal. This significantly reduces the difficulty of the thermal analysis, where a “lumped capacitance model” can be used with good accuracy.

In a lumped capacitance model, temperature equilibrates with the surrounding gas in an exponential manner:

$$\frac{T - T_\infty}{T_i - T_\infty} = \exp\left[-\left(\frac{hA}{\rho V C_p}\right)t\right] \quad (2)$$

where T_∞ is the stream temperature, T_i is the initial temperature of the window, ρ is the polyimide density and C_p is the polyimide heat capacity. This equation would be especially easy to solve, except for the fact that the heat capacity of polyimide changes significantly as it heats from its cryogenic starting point [6] (see Figure 9). This necessitates a time-dependent solution.

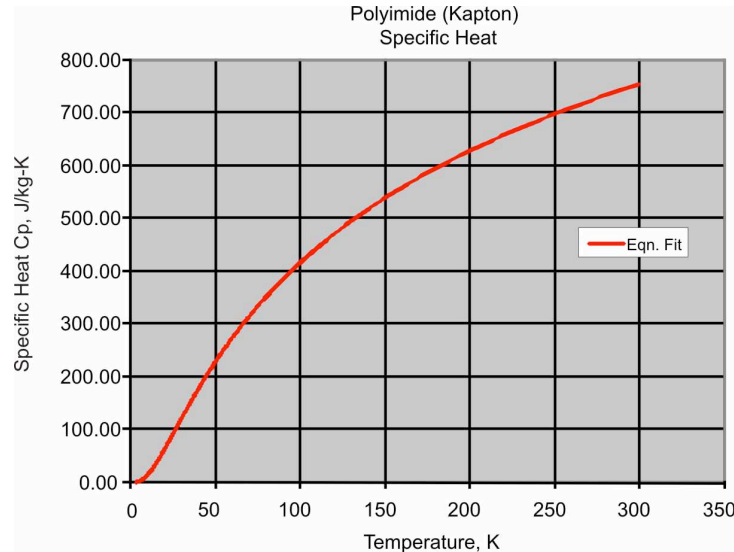


Figure 9. Polyimide specific heat (J/kg-K)

According to DuPont [7], Kapton has been used successfully up to 400 °C. It does not melt; rather it decomposes at about 500 C. So the failure criterion is somewhere in the range of 675-775 K. The time allowed to reach this temperature depends on assumptions on the conditions along the trajectory of the target. We assume that an aperture near the chamber wall can effectively protect gas in the target delivery tube, such that the time within the chamber is approximately 25 ms (a path length of 5 m at 200 m/s).

Comsol was used to solve the 1D transient heating of polyimide with temperature-dependent properties. Figure 10 shows a result with an assumed $25 \text{ W/m}^2\text{K}$ heat transfer coefficient and no radiation heat transfer. At 25 ms, the temperature reaches $\sim 650 \text{ K}$, which is marginally below the failure criterion. As can be seen by inspection of equation 2, the heating rate depends linearly on the window thickness in this regime where the lumped capacitance model is valid. Increasing the thickness of the window is an effective means to slow the heat-up.

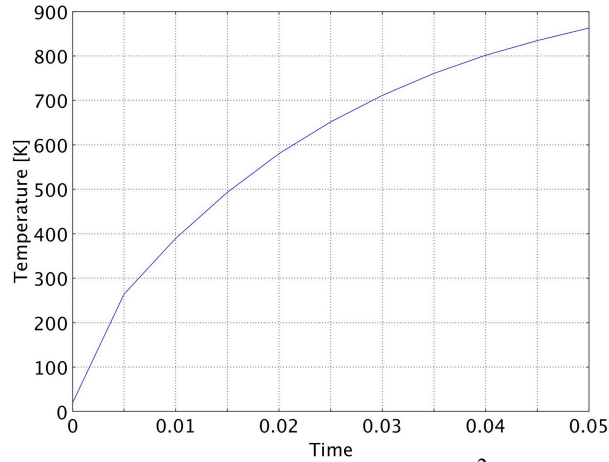


Figure 10. Heat-up of the polyimide window with $h=25 \text{ W/m}^2$ and no radiation

The effect of radiation

We explored several scenarios in which radiation plays a role in the heat transfer to the LEH window. We varied the emissivity of the polyimide, which is not well known, and included radiation from the window to the hohlraum interior (assumed to remain at 20 K). For example, Figures 11 and 12 show the effect of reducing the polyimide emissivity from 1.0 to 0.1, which can be obtained easily with a thin coating of gold on the window (note, a similar technique used in HAPL achieved a reflectivity of over 98% in a 1000-K chamber using a 10 nm coating of gold on the capsule surface). Clearly reducing radiation heat transfer is a critical requirement for the survival of the LEH window.

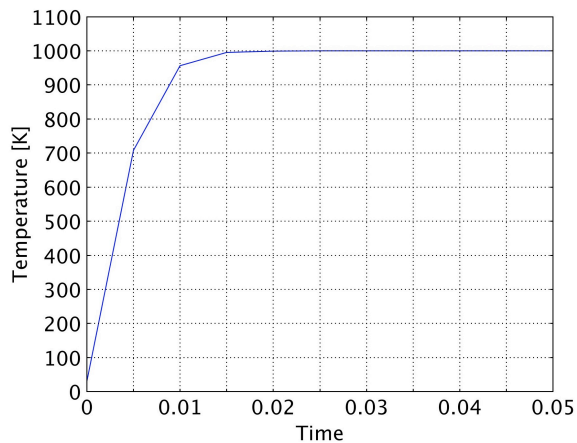


Figure 11. Window heating with $h=25 \text{ W/m}^2\text{-K}$ and $\epsilon=1.0$

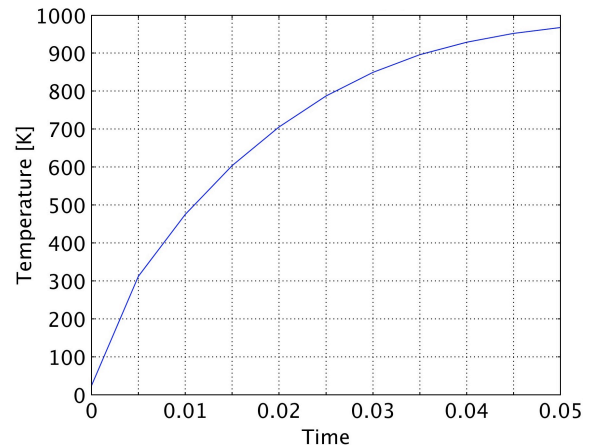


Figure 12. Window heating with $h=25 \text{ W/m}^2\text{-K}$ and $\epsilon=0.1$

Evaluation of target spinning

Differences in the heat transfer around the hohlraum may result from spinning (“rifling”). A typical high-power rifle bullet travels at 1000 m/s and spins at 300,000 rpm. Scaling this to our 200 m/s case while maintaining the same ratio of spin rate to injection velocity, we estimate a maximum spin of 60,000 rpm and circumferential velocity of 20 m/s on the hohlraum lateral surface. According to Ron Petzoldt, 12,000 rpm is a reasonable value chosen to avoid excessive stress on the DT and still provide adequate stabilization. This is 5 times slower than a high-power rifle, and leads to only 4 m/s spin velocity on the hohlraum lateral surface. Compared with the 200 m/s longitudinal velocity, we believe the effect on heat transfer will be negligible. In any case, heat transfer to the Pb hohlraum walls is not a significant problem due to the higher heat capacity and lower heat transfer coefficient.

Hohlraum shaping

DS2V was used to explore the possible improvements to heat transfer by shaping the hohlraum slightly. For example, the sharp corners of the hohlraum produce a high velocity region and peak heat transfer coefficients at the location of the corners. We asked ourselves whether some rounding of the corners might improve this. The graphical results for flow speed are nearly indistinguishable from the square-edged hohlraum. The heat transfer coefficient is shown in Figure 13. Little if any improvement is observed.

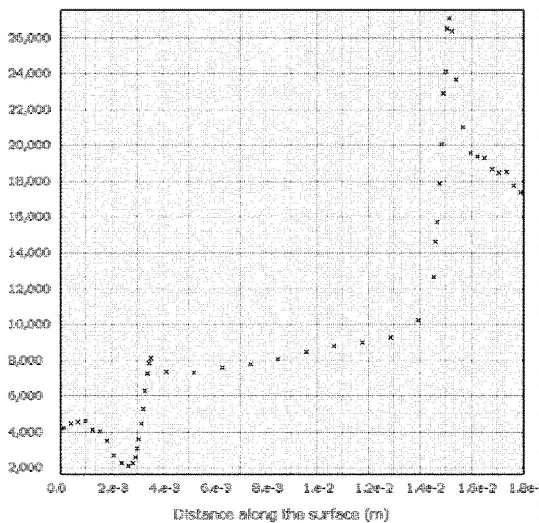


Figure 13. Heat transfer around the surface of the hohlraum with rounded corners

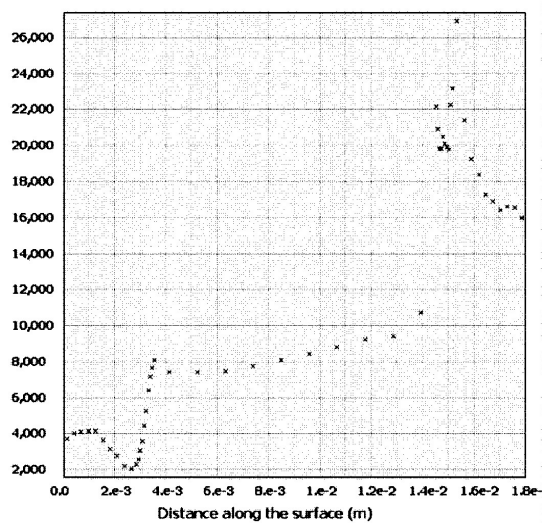


Figure 14. Heat transfer around the surface of the hohlraum with front side depression

Since the back of the target (in the wake) exhibits much lower heat flux, it seemed likely that some shaping of the front surface may trap gas and provide a kind of “buffer” to reduce heat transfer. Figure 14 shows the resulting heat transfer coefficient with a shallow curvature on the front surface. The heat transfer decreased very modestly, from 1.8 to 1.6 W/cm². This is probably not worth the effort.

References

- [1] Gwen Loosmore and Peter Amendt, "LIFE Target Details," LLNL internal document, April 22, 2009.
- [2] J. Latkowski, "Target Concepts" (powerpoint presentation), July 13, 2009.
- [3] G. A. Bird, "Visual DSMC Program for Two-Dimensional and Axially Symmetric Flows: The DS2V Program User's Guide Version 3.8," October 2006.
- [4] Frank Incropera and David DeWitt, "Fundamentals of Heat and Mass Transfer, Fourth Edition," John Wiley and Sons, 1996.
- [5] M. Jakob, *Heat Transfer*, Vol 1. Wiley, New York, 1949.
- [6] NIST Cryogenic Technologies Group, "Material Properties: Polyimide (Kapton)", http://cryogenics.nist.gov/MPropsMAY/Polyimide%20Kapton/PolyimideKapton_rev.htm
- [7] http://www2.dupont.com/Kapton/en_US/